Luo et al. *Zool. Res.* 2021, 42(5): 592−605
https://doi.org/10.24272/j.issn.2095-8137.2021.079

ZR | Zoological Research

Article Open Access

Scavenging reactive oxygen species is a potential strategy to protect *Larimichthys crocea* against environmental hypoxia by mitigating oxidative stress

Sheng-Yu Luo[1], Cheng Liu[1], Jie Ding[1], Xin-Ming Gao[1], Jing-Qian Wang[1], Yi-Bo Zhang[1], Chen Du[1], Cong-Cong Hou[1], Jun-Quan Zhu[1,*], Bao Lou[2,*], Xiong-Fei Wu[3], Wei-Liang Shen[3]

[1] *Key Laboratory of Applied Marine Biotechnology by the Ministry of Education*, *School of Marine Sciences*, *Ningbo University*, *Ningbo*, *Zhejiang* 315211, *China*

[2] *Zhejiang Academy of Agricultural Sciences*, *Hangzhou*, *Zhejiang* 310021, *China*

[3] *State Key Laboratory of Large Yellow Croaker Breeding*, *Ningbo Academy of Oceanology and Fishery*, *Ningbo*, *Zhejiang* 315012, *China*

ABSTRACT

The large yellow croaker (*Larimichthys crocea*), which is an economically important mariculture fish in China, is often exposed to environmental hypoxia. Reactive oxygen species (ROS) homeostasis is essential for the maintenance of normal physiological conditions in an organism. Direct evidence that environmental hypoxia leads to ROS overproduction is scarce in marine fish. Furthermore, the sources of ROS overproduction in marine fish under hypoxic stress are poorly known. In this study, we investigated the effects of hypoxia on redox homeostasis in *L. crocea* and the impact of impaired redox homeostasis on fish. We first confirmed that hypoxia drove ROS production mainly via the mitochondrial electron transport chain and NADPH oxidase complex pathways in *L. crocea* and its cell line (large yellow croaker fry (LYCF) cells). We subsequently detected a marked increase in the antioxidant systems of the fish. However, imbalance between the pro-oxidation and antioxidation systems ultimately led to excessive ROS and oxidative stress. Cell viability showed a remarkable decrease while oxidative indicators, such as malondialdehyde, protein carbonylation, and 8-hydroxy-2 deoxyguanosine, showed a significant increase after hypoxia, accompanied by tissue damage. N-acetylcysteine (NAC) reduced ROS levels, alleviated oxidative damage, and improved cell viability *in vitro*. Appropriate uptake of ROS scavengers (e.g., NAC and elamipretide Szeto-Schiller-31) and inhibitors (e.g., apocynin, diphenylene iodonium, and 5-hydroxydecanoate) may be effective at overcoming hypoxic toxicity. Our findings highlight previously unstudied strategies of hypoxic toxicity resistance in marine fish.

Keywords: Dissolved oxygen; Redox

Received: 10 June 2021; Accepted: 10 August 2021; Online: 11 August 2021

Foundation items: This work was supported by the NSFC-Zhejiang Joint Fund for the Integration of Industrialization and Informatization (U1809212), Scientific and Technical Project of Zhejiang Province (2016C02055-7), Scientific and Technical Project of Ningbo City (2021Z002, 2015C110005), Ningbo Science and Technology Plan Projects (2018A610228), Teaching and Research Project of Ningbo University (XYL19023), Collaborative Innovation Center for Zhejiang Marine High-efficiency and Healthy Aquaculture, K.C. Wong Magna Fund in Ningbo University

*Corresponding authors, E-mail: zhujunquan@nbu.edu.cn; loubao6577@163.com

homeostasis; Antioxidant system; N-acetylcysteine

INTRODUCTION

Dissolved oxygen (DO), i.e., molecular oxygen dissolved in water, is the primary source of oxygen for most aquatic organisms. Unlike the terrestrial environment, hypoxia with DO<2 mg/L occurs frequently in aquatic ecosystems (Diaz, 2001) due to contamination, high-density fish breeding, algal blooms, and elevated temperatures (Mahfouz et al., 2015). Of concern, both the frequency and severity of hypoxia in marine environments are expected to increase under climate change (Breitburg et al., 2018). Environmental hypoxia can disturb homeostasis in fish, resulting in reduced food intake, growth rate, and fertility, and even death (Martínez et al., 2011; Schulte, 2014).

Stressors, including hypoxia, can induce the overproduction of reactive oxygen species (ROS), such as hydrogen dioxide (H_2O_2), superoxide anion ($O_2^{\bullet-}$), and hydroxyl radicals (•OH), in aerobic organisms (Leonarduzzi et al., 2010). ROS are produced by the mitochondrial electron transport chain (ETC) (Sommer et al., 2010), cytochrome P450 system (Leung & Nieto, 2013), heme protein auto-oxidation (Almeida et al., 2015), NADPH oxidase (NOX) complex (DeCoursey, 2016), xanthine oxidase (XO) (Meneshian & Bulkley, 2002), nitric oxide synthases (NOS) (Pacher et al., 2007), and fatty acid β-oxidation within peroxisomes (Fransen et al., 2012). The mitochondrial mechanism of ROS production involves electrons escaping from the ETC and reacting with O_2 to produce $O_2^{\bullet-}$ (Brownlee, 2005; Jastroch et al., 2010). In contrast, NOXs sequentially transfer electrons from NADPH to flavin adenosine dinucleotide (FAD), heme groups, and then to molecular oxygen, producing superoxide (Gimenez et al., 2016). In higher animals, the ETC (Hernansanz-Agustín et al., 2017) and NOX complex (Lu et al., 2012) are sources of excess ROS under hypoxic stress. However, studies on the origins of ROS in marine fish under environmental hypoxia remain scarce.

Corresponding to ROS production, organisms possess integrated antioxidant defense systems to help regulate cellular ROS homeostasis. These defense systems consist of enzymatic antioxidants, such as superoxide dismutase (SOD), catalase (CAT), glutathione peroxidase (GPx), peroxidase (POD), glutathione S-transferase (GST), and glutathione reductase (GR), and non-enzymatic antioxidant molecules, such as reduced glutathione (GSH), uric acid, ascorbic acid, and carotenes (Guérin et al., 2001; Ming et al., 2019). If excessive ROS are not counteracted by the antioxidant defense system, they will promptly attack major cellular macromolecules, including lipids, proteins, and DNA, resulting in the production of malondialdehyde (MDA), protein carbonyls (PCO), and 8-hydroxy-2 deoxyguanosine (8-OHdG), as well as cell function loss, apoptosis, and necrosis (Holowiecki et al., 2017; Klein & Ackerman, 2003).

The large yellow croaker (*Larimichthys crocea*) is an economically and nutritionally important mariculture fish, with an annual yield of 225 549 tons in China in 2019 (Fishery Administration of the Ministry of Agriculture and Rural Areas et al., 2020). However, the frequent occurrence of the "floating head" phenomenon due to environmental hypoxia has seriously reduced farming efficiency and become a major constraint hindering the *L. crocea* fishery industry (Liu et al., 2018). Thus, exploring the mechanism underlying hypoxic stress-adaptation strategies in *L. crocea* is essential, starting with the redox homeostasis regulation mechanism. Nevertheless, research on the redox regulatory system in *L. crocea* in response to hypoxia is relatively scarce. We previously showed that acute hypoxia enhances SOD and CAT activity in *L. crocea* (Wang et al., 2017), indicating that the enzymatic antioxidant system plays a crucial role in hypoxia-stressed *L. crocea*. In the present study, we first examined whether hypoxia induces excessive ROS production and determined the main sources of ROS in *L. crocea* under hypoxic conditions. Second, we tested the responses of the antioxidant defense system to hypoxia-induced ROS overproduction. Third, we identified organism/cell fate when the redox homeostasis regulation system is insufficient to withstand excessive ROS. Furthermore, we explored whether ROS eliminators and inhibitors can reverse oxidative stress and cell viability decline caused by hypoxia using an *in vivo* hypoxia model. Our findings could be used to improve hypoxic tolerance in marine fish.

MATERIALS AND METHODS

Fish experiments and sample collection

We obtained *L. crocea* (length 15.90±1.52 cm, body weight 63.61±6.63 g) from Fufa Aquatic Products Co., Ltd. (Ningde, China). The fish were domesticated under normoxic conditions (DO 8.0–8.5 mg/L) for two weeks prior to the experiment. A total of 240 fish were randomly divided into six toughened plastic tanks (800 L each). Three tanks were used as the hypoxia-treated groups (HTGs) and three tanks were used as the normoxia-control groups (NCGs). For the HTGs, the DO in each tank was adjusted to 2.0 mg/L within 10 min of starting the experiment by injecting nitrogen, and was then maintained at 2.0±0.1 mg/L for 96 h. For the NCGs, treatment was consistent with the domestication conditions. A HACH DO probe system (HACH LDO II, HACH, USA) was used to monitor and maintain DO in real time. Samples were collected at 0, 6, 24, 48, and 96 h after starting the experiment. At each time point, three fish were taken from each tank and dissected on an ice-covered tray. Dissected gill and liver samples were frozen in liquid nitrogen and stored at −80 °C. The principles and procedures of sampling were in strict accordance with the requirements of the Governing Regulation for the Use of Experimental Animals in Zhejiang Province (Zhejiang Provincial Government Order No. 263, released 17 August 2009, effective from 1 October 2010) and were approved by the Animal Care and Use Committee of Ningbo University.

Cell culture and hypoxic challenge

The large yellow croaker fry (LYCF) cell line was kindly provided by Dr. You-Hua Huang, South China Agricultural University. The LYCF cells were cultured in Leibovitz's-15 Medium (Gibco, USA) supplemented with 10% (v/v) fetal bovine serum (Gibco, USA) and 200 μg/mL of penicillin-

streptomycin (Gibco, USA) at 27 °C. For the normoxic conditions, the cells were cultured in an incubator. For the hypoxic treatments, the cells were cultured under hypoxic conditions at 1% O_2 and 99% N_2 in a MIC-101 modular incubator (Billups Rothenberg, USA) for 0, 1, 3, 6, 12, 24, and 48 h. For the ROS modification experiments, the functions and concentrations of ROS scavengers (N-acetylcysteine (NAC) and elamipretide Szeto-Schiller-31 (SS-31)) and inhibitors (apocynin, diphenylene iodonium (DPI), and 5-hydroxydecanoate (5-HD)) are shown in Table 1. The following experimental groups were established: normoxia, hypoxia, hypoxia+NAC, hypoxia+DPI, hypoxia+apocynin, hypoxia+SS-31, hypoxia+5-HD, and hypoxia+apocynin+5-HD. All modulators were added to the medium 1 h prior to hypoxic stress.

Measurement of intracellular and mitochondrial ROS

The levels of intracellular ROS were determined using 2',7'-dichlorofluorescein diacetate (DCFH-DA, Sigma, USA) and dihydroethidium (DHE; Beyotime, China) detection as well as H_2O_2 and superoxide assay kits (Beyotime). For fluorescence probe DCFH-DA and DHE detection, we proceeded as follows: (1) Diluted DCFH-DA and DHE to final concentrations of 10 μmol/L and 0.5 μmol/L, respectively, with serum-free medium; (2) Removed the cell culture and added 1 mL of diluted fluorescence probe to one well of a six-well plate; (3) Incubated the cells at 27 °C for 20 min; (4) Incubated the cells with 1×Hoechst 33342 (Beyotime) at 27 °C for 5 min to label the nucleus; and (5) Photographed the cells with a laser confocal microscope (LSM880, Carl Zeiss, Germany) and measured fluorescence intensity with a FACSCalibur flow cytometer (Becton Dickinson, USA) or a fluorescence microplate reader (Varioskan Flash, Thermo Fisher Scientific, USA). The H_2O_2 assay kit was used to measure intracellular H_2O_2 levels in the cell lysate, culture supernatant, and liver tissue supernatant. The superoxide assay kit was applied to measure intracellular superoxide in the LYCF cells.

The MitoSOX Red mitochondrial superoxide indicator (Yeasen, China) was used to trace mitochondrial ROS. The procedure was the same as for fluorescence probe DCFH-DA and DHE detection, except that the working concentration of the MitoSOX Red mitochondrial superoxide indicator was 2.5 μmol/L and the incubation conditions were 20 min at 27 °C.

Detection of antioxidative indicators

To examine the responses of the antioxidant system in *L. crocea*, we detected the total antioxidant capacity (T-AOC), SOD, CAT, POD, GPx, GST, and GR enzyme activity, and GSH and glutathione disulfide (GSSG) levels *in vivo* and *in vitro* using appropriate assay and content detections kits for T-AOC, total SOD, CAT, total GPx (Beyotime), GST, GR (Solarbio, China), peroxidase (Nanjing Institute of Bioengineering, China), GSH, and GSSG (Solarbio, China) according to the manufacturers' instructions. The fluorescent probe naphthalene-2,3-dicarboxaldehyde (NDA) was used to assess GSH levels in the LYCF cells. In brief, 1 mL of NDA diluted with serum-free medium to a final concentration of 500 μmol/L was added to one well of a six-well plate and incubated at 27 °C for 30 min. The cells were washed twice with phosphate-buffered saline and then observed with a confocal microscope or analyzed with a flow cytometer.

Determination of oxidative stress markers MDA, PCO, and 8-OHdG

The levels of lipid peroxide MDA, protein oxidative indicator PCO, and DNA oxidative marker 8-OHdG were measured *in vivo* and *in vitro* using an MDA kit (Nanjing Institute of Bioengineering), PCO content detection kit (Solarbio, China), and fish 8-OHdG ELISA kit (Chenglinbio, China), respectively, in accordance with the manufacturers' instructions.

Histological and cellular lesion analysis

For histological analysis, gill and liver tissue samples from fish in the NCGs and HTGs were sampled at 96 h, cut into cubes, and fixed for 24 h in Bouin's fixative. Subsequently, the samples were rinsed in 70% ethanol for 48 h, dehydrated in a graded ethanol series, embedded into paraffin blocks, sectioned at 5 μm thickness, stained with hematoxylin and eosin, and then observed under an optical microscope (Olympus BX51; Olympus, Japan). For ultrastructural analysis, sample preparation and staining were performed according to Oró et al. (2016). The sections were examined and photographed with a transmission electron microscope (TEM; H-7650; Hitachi, Japan).

Cell viability assay

Cell viability was evaluated using a cell counting kit (CCK-8; MedChem Express, USA) according to the manufacturer's instructions. In brief, cells were plated in 96-well plates at a concentration of 1×10^4 cells per well. After treatment, 10 μL of CCK-8 reagent was added to each well and allowed to react for 2 h. Absorbance at 450 nm was measured with a microplate reader (SPECTRA MAX 190; Molecular Devices, USA).

Comparative transcriptome analysis

Total RNA was extracted from liver and gill tissues sampled at 0, 6, 24, 48, and 96 h after exposure to hypoxic stress using TRIzol reagent (Invitrogen, China) according to standard protocols. The integrity, purity, and concentration of each RNA sample were validated, as described in our previous study (Ding et al., 2020). Equal amounts of RNA isolated from the livers and gills of six individuals at each time point were

Table 1 ROS modulators used in this study and their working concentrations

Modulator	Function	Working concentration (μmol/L)
NAC	ROS scavenger	1 000
5-HD	Mitochondrial ROS-specific inhibitor	100
SS-31	Mitochondrial ROS-specific scavenger	5
Apocynin	Inhibitor of NOX-derived ROS, blocking assembly of NOX complexes	100
DPI	Inhibitor of NOX-derived ROS, inhibiting activity of NOX subunits	1

pooled and used for library construction. The cDNA libraries prepared from gill and liver tissues of fish exposed to different hypoxic durations were labeled Gi-0h, Gi-6h, Gi-24h, Gi-48h, Gi-96h, Li-0h, Li-6h, Li-24h, Li-48h, and Li-96h, respectively. Sequencing library construction and transcriptome sequencing were conducted using the Illumina HiSeq 2500 platform at Beijing BioMarker Technologies (China) following the manufacturer's instructions. Data filtering, reference genome sequence mapping (accession No.: PRJNA354443), and transcript expression calculation were conducted using BMKCloud (www.biocloud.net). Differential expression analysis was performed using the EBseq R package (Leng et al., 2013). Significant differential expression thresholds were set to P<0.05 and $|\log_2(\text{fold-change})|\geq 1$. The differentially expressed transcripts (DETs) were aligned to the Nr, GO, Swiss-Prot, KEGG, KOG, eggNOG, COG, and Nt databases. Candidate DETs potentially associated with oxidative stress and cellular redox regulation were identified based on enrichment analyses, annotations, manual literature searches, and real-time quantitative polymerase chain reaction (RT-qPCR) experiments.

RT-qPCR

To validate the reliability of the expression data obtained from transcriptome sequencing in *L. crocea*, we analyzed the transcript expression patterns of 10 genes involved in redox regulation based on RT-qPCR using a LightCycler 480 instrument (Roche, Switzerland). The primers used for RT-qPCR are listed in Supplementary Table S1. cDNA synthesis and RT-qPCR analysis were performed as described previously (Luo et al., 2019).

Statistical analysis

Data are expressed as mean±standard error of the mean (*SEM*). All statistical analyses were carried out using SPSS v21.0 (IBM, USA). Significant differences between two groups were determined using the two-tailed independent samples *t*-test. Significant differences between three or more groups were determined using one-way analysis of variance (ANOVA), followed by Tukey's *post hoc* test. For all line charts and histograms, "*" indicates a significant difference (P<0.05) compared with another set of data and "**" indicates an extremely significant difference (P<0.01).

RESULTS

Hypoxia drives overproduction of ROS both *in vivo* and *in vitro*

We used *in vivo* and *in vitro* hypoxia models to investigate whether hypoxia can increase the level of ROS in large yellow croaker cells. Results showed that the fluorescence intensities of ROS (Figure 1A) and $O_2^{\bullet-}$ (Figure 1F) in LYCF cells were markedly increased after hypoxia treatment. Mean fluorescence intensity (MFI) of the ROS indicator increased substantially after 12, 24, and 48 h of hypoxia treatment (Figure 1C–E). Analogously, the MFI of the $O_2^{\bullet-}$ indicator increased after 24 h of hypoxia treatment (Figure 1G). Fluorescence microplate reader measurements also showed a marked increase in DCFH-DA-labelled intracellular ROS levels in LYCF cells exposed to hypoxia (Figure 1H). Intracellular superoxide levels were elevated in a time-dependent pattern (Figure 1I). In addition, H_2O_2 levels in the liver, LYCF cells, and culture supernatant increased significantly following environmental hypoxia treatment (Figure 1J–L).

Excessive ROS induced by hypoxia is mainly derived from mitochondrial ETC and NOX complex pathways

There are multiple sources of ROS in cells under stress or pathological conditions. To determine whether mitochondria are the source of ROS in LYCF cells under hypoxic conditions, we detected the levels of mitochondrial ROS in LYCF cells and observed a time-dependent enhancement in the fluorescence intensity of MitoSOX RED (Figure 2A). To verify the sources of excessive ROS, we pretreated the cells with NAC, SS-31, 5-HD, apocynin, and DPI separately or in different combinations prior to hypoxia treatment.

Compared with the hypoxia group, ROS and superoxide levels in the cells of the hypoxia+NAC, hypoxia+DPI, hypoxia+apocynin, hypoxia+SS-31, and hypoxia+5-HD groups were significantly lower, indicating that all five ROS regulators could reduce ROS levels in LYCF cells under hypoxic stress. In addition, although ROS and superoxide levels were significantly lower in the hypoxia+apocynin and hypoxia+5-HD groups compared to the hypoxia group, they were still significantly higher than those in the normoxia group, indicating that separate inhibition of ROS by the NOX complex and mitochondrial ETC sources significantly reduced ROS and superoxide levels in LYCF cells under hypoxic stress. The levels of ROS and superoxide in the hypoxia+apocynin+5-HD-treated cells did not differ significantly from levels in the normoxia group, indicating that ROS and superoxide levels in LYCF cells recovered to normoxia control levels after inhibition of NOX complex- and mitochondrial ETC-derived ROS under hypoxic stress (Figure 2B, C).

High-level ROS stimulates antioxidant system *in vivo* and *in vitro*

In both liver and LYCF cells, T-AOC (Figure 3A, B) and SOD (Figure 3C, D), CAT (Figure 3E, F), POD (Figure 3G, H), GPx (Figure 3I, J), GST (Figure 3K, L), and GR activities (Figure 3M, N) were activated by hypoxia. In contrast, GSH was depleted in a time-dependent manner (Figure 3O, P), accompanied by a gradual rise in GSSG levels (Figure 3S, T). Correspondingly, the GSH/GSSG ratio was gradually attenuated (Figure 3U, V). Data generated from the NAD labeling experiments also showed a significant decrease in intracellular GSH levels after 24 h of hypoxia treatment (Figure 3Q, R).

RNA sequencing (RNA-seq) and RT-qPCR analyses confirm initiation of redox regulatory system

To examine whether hypoxia affects the expression of genes related to ROS homeostasis, we performed comparative transcriptome analysis on the liver and gills of *L. crocea* exposed to hypoxic stress for 0, 6, 24, 48, and 96 h. We screened 536 DETs involved in cellular redox homeostasis (Supplementary Table S2). Based on the functional importance of the annotated DETs, we generated a shortlist of 76 crucial transcripts encoding antioxidant enzymes (Figure 4A), proteins related to ROS generation (Figure 4B),

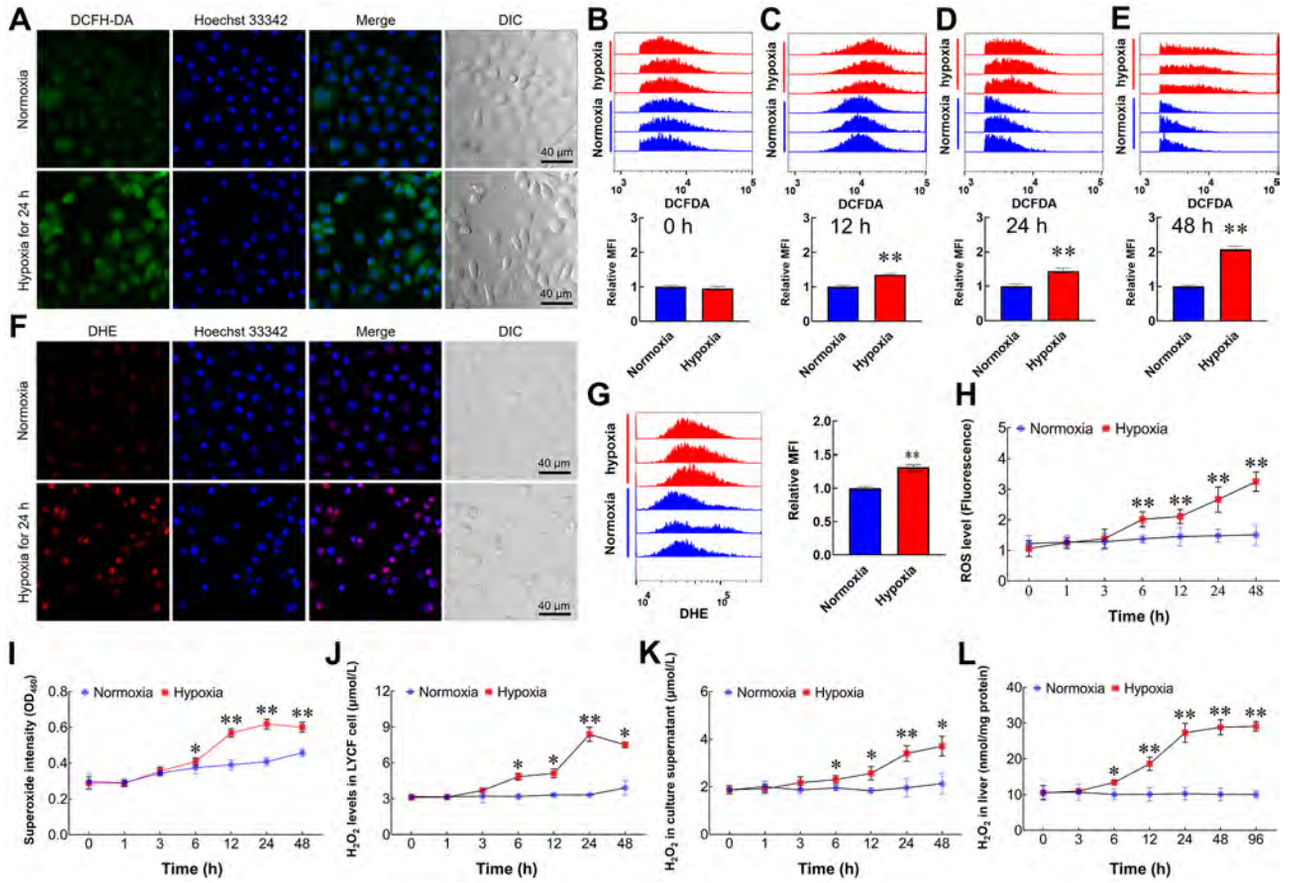

Figure 1 Hypoxia induces an increase in ROS levels

A: Representative fluorescence photomicrographs of ROS levels (green) in LYCF cells with/without hypoxia for 24 h. DIC: Differential interference contrast. B–E: FACS analysis of ROS levels in LYCF cells with/without hypoxia for 0, 12, 24, and 48 h, respectively. MFI: Mean fluorescent intensity. F: Representative fluorescence photomicrographs of $O_2^{\bullet-}$ levels (red) in LYCF cells with/without hypoxia for 24 h. G: FACS analysis of $O_2^{\bullet-}$ levels in LYCF cells with/without hypoxia for 24 h. H: Fluorescence microplate reader measurement of changes in intracellular ROS levels (fluorescence OD value) in LYCF cells with/without hypoxia. I: Superoxide assay of changes in intracellular superoxide levels in LYCF cells with/without hypoxia. J–L: H_2O_2 assay of changes in H_2O_2 levels in LYCF cells, culture supernatant, and liver, respectively. *: P<0.05; **: P<0.01.

and redox-regulatory factors (Figure 4C). After hypoxia treatment, most transcripts encoding antioxidant enzymes were up-regulated (Figure 4A), most transcripts encoding ROS production-related proteins were moderately up-regulated (Figure 4B), and most transcripts encoding redox-regulatory factors were markedly down-regulated (Figure 4C). The expression levels of 10 redox-related transcripts were analyzed by RT-qPCR. Notably, among these 10 genes, the expression levels of *gpx3*, *mgst1*, *mgst2*, and *mgst3* were significantly induced in the liver by hypoxia (Figure 4D). The gene expression data obtained by RT-qPCR and the RNA-seq data were highly consistent (Figure 4D) and strongly correlated, with a Pearson correlation coefficient of 0.9228 (Figure 4E). These results confirmed the reproducibility and reliability of the RNA-seq data.

Redundant ROS attack biomacromolecules, resulting in histopathological changes and cellular lesions

To further verify the effects of excessive ROS, we evaluated the MDA, PCO, and 8-OHdG levels using *in vivo* and *in vitro* models. With increasing duration of hypoxic stress, MDA (Figure 5A, B), PCO (Figure 5C, D), and 8-OHdG (Figure 5E, F) levels in both liver and LYCF cells increased markedly compared with levels in the normoxia group. Histopathological and ultrastructural analyses were performed to examine the effects of environmental hypoxic stress on tissue and cell morphology in *L. crocea*. Gill sections from the NCGs showed typical structures, with secondary lamellae (SL) on the sides of gill filaments arranged in parallel arrays with normal pillar cells (PCs) and epithelial cells (EPs) (Figure 5G–J). After 96 h of exposure to hypoxia, partial gill lesions were observed in the HTGs, including vacuolation in some PCs, fewer hemocytes (HCs) in the efferent and afferent branchial arteries (EBA and ABA), detachment of EPs from SL, and partial fusion of SL (Figure 5K–N). The NCG liver sections showed normal, compactly arranged hepatocytes and vessels filled with normally shaped HCs (Figure 5O, Q). Following 96 h of hypoxia treatment, the hepatic tissues showed some pathological characteristics in several areas. For example, HCs in some blood vessels were unevenly distributed and stacked together; the shape of HCs and their nuclei changed from rounded to elongated (Figure 5P); and the pancreas

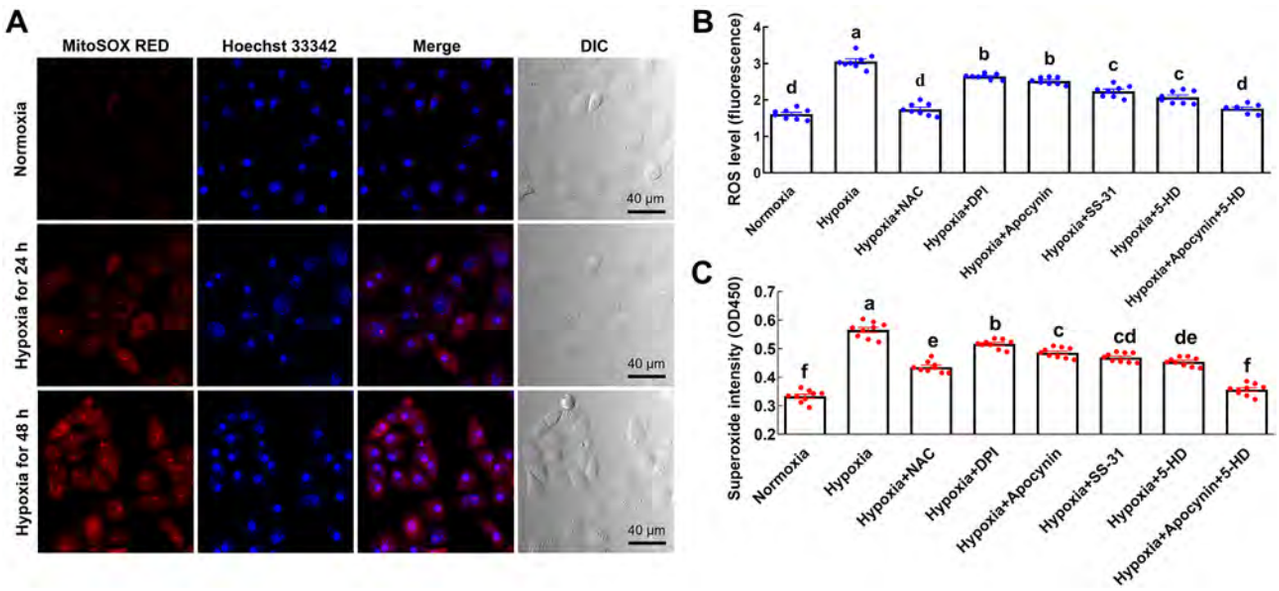

Figure 2 Hypoxia-induced excessive ROS is mainly derived from mitochondrial ETC and NOX pathways

A: Representative fluorescence photomicrographs of mitochondrial superoxide levels (red) in LYCF cells with/without hypoxia for 24 and 48 h. B: Fluorescence microplate reader measurement of changes in intracellular ROS levels (fluorescence OD value) in LYCF cells with/without hypoxia and/or NAC, DPI, apocynin, SS-31, 5-HD, or their combination for 24 h. C: Superoxide assay of intracellular superoxide levels in LYCF cells with/without hypoxia and/or NAC, DPI, apocynin, SS-31, 5-HD, or their combination for 24 h. Different letters on bars represent statistically significant intergroup differences.

partially swelled, and the number of HCs increased, showing characteristics of congestion (Figure 5R). A normal hepatic ultrastructure, characterized by clustered formation of mitochondria with clear cristae and rounded and central nuclei and nucleoli, was observed in the NCGs (Figure 5S, T). Hepatocytes from the HTGs showed some pathological characteristics, such as regressed mitochondrial cristae (resulting in mitochondrial vacuolation), nucleus deformation, and uneven chromatin distribution (Figure 5U, V).

NAC eliminates excessive ROS in LYCF cells and alleviates oxidative toxicity

Given the oxidative effects of hypoxia-induced ROS, we further explored whether ROS eliminator NAC can mitigate the oxidative toxicity caused by hypoxia in LYCF cells. We found that NAC effectively alleviated the reduction in cell viability caused by hypoxia treatment, and the effect was most pronounced at a concentration of 1 mmol/L NAC (Figure 6I). The fluorescence intensity of ROS, $O_2^{\bullet-}$, and mitochondrial superoxide in cells increased after hypoxia treatment, but the effects were reversed by NAC pretreatment (Figure 6A). Analogously, quantitative fluorescence-activated cell sorting (FACS) analysis revealed that NAC pretreatment effectively alleviated the increase in ROS and $O_2^{\bullet-}$ levels after 24 h of hypoxia treatment (Figure 6B, C). As expected, the levels of H_2O_2 (Figure 6D), superoxide (Figure 6E), MDA (Figure 6F), PCO (Figure 6G), and 8-OHdG (Figure 6H) in the NAC+hypoxia group were lower than the levels in the hypoxia group.

DISCUSSION

Whether hypoxia can induce ROS generation remains controversial, as a decrease in ROS levels can be easily explained by decreased substrate (oxygen) availability and an increase in ROS during hypoxia seems counterintuitive (Sommer et al., 2016). However, among the various studies investigating this issue, most support the paradox that hypoxia enhances ROS production (Balogh et al., 2019; Guzy et al., 2005; Waypa et al., 2001). Studies on hypoxic stress-induced overproduction of ROS have also been reported in fish. For example, Rahman & Thomas (2011) detected a significant increase in $O_2^{\bullet-}$ levels in the livers of *Micropogonias undulatus* after 4 weeks of chronic hypoxic stress. Baldissera et al. (2020) examined ROS levels in the gills of catfish (*Lophiosilurus alexandri*) after 72 h of hypoxic stress using DCFH-DA fluorescent probes and showed that ROS levels were significantly higher than levels in the normoxia group. These studies support the view that hypoxia induces significant ROS production. Similarly, we examined ROS levels in *L. crocea* liver samples and LYCF cells after hypoxic stress using corresponding biochemical kit assays and fluorescent probes. Results showed that H_2O_2 levels in the livers of the hypoxia group were significantly higher than those in the normoxia group. The intracellular $O_2^{\bullet-}$, mitochondrial $O_2^{\bullet-}$, H_2O_2, and superoxide levels in hypoxic LYCF cells were also significantly higher than those in the normoxia group, indicating environmental hypoxia induces the overproduction of multiple ROS in *L. crocea*, thus favoring the paradox mentioned above. However, the underlying mechanisms require further investigation.

Studies in mammals have shown that the ETC and NOX complex are the sources of excess ROS in organisms exposed to hypoxic stress. Hernansanz-Agustín et al. (2017) found that elevated $O_2^{\bullet-}$ in bovine aortic endothelial cells under

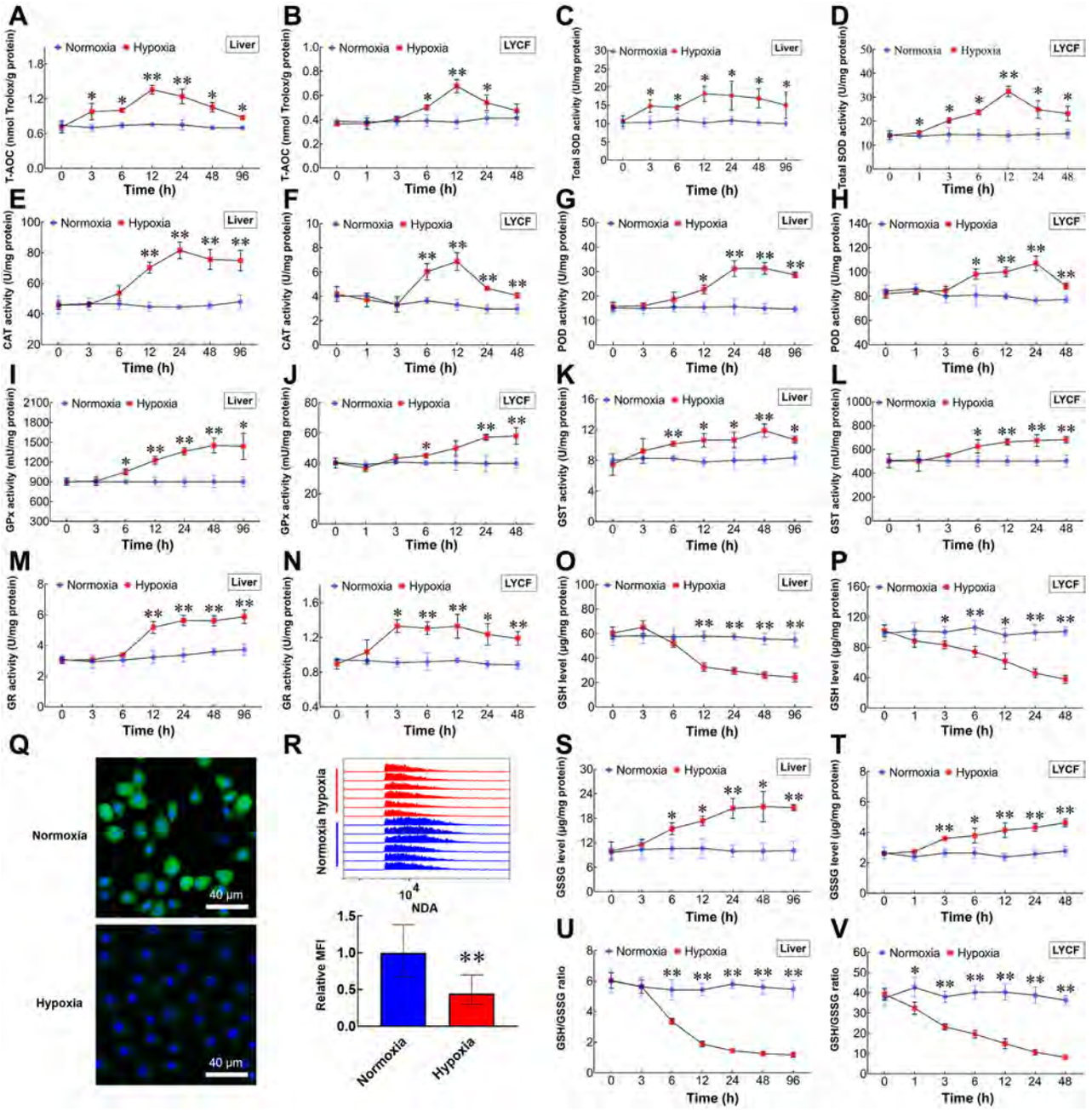

Figure 3 Increased ROS drives antioxidant system in *L. crocea* and LYCF cells under hypoxic conditions

A, B: T-AOC assay of changes in T-AOC in liver and LYCF cells with/without hypoxia. C, D: Total SOD activity assay of changes in SOD activity in liver and LYCF cells with/without hypoxia. E, F: Changes in CAT activity in liver and LYCF cells with/without hypoxia. G, H: Changes in POD activity in liver and LYCF cells with/without hypoxia. I, J: Changes in total GPx activity in liver and LYCF cells with/without hypoxia. K, L: Changes in total GST activity in liver and LYCF cells with/without hypoxia. M, N: Changes in GR activity in liver and LYCF cells with/without hypoxia. O, P: Changes in GSH level in liver and LYCF cells with/without hypoxia. Q: Representative fluorescence photomicrographs of GSH level (green) in LYCF cells with/without hypoxia for 24 h. R: FACS analysis of GSH levels in LYCF cells with/without hypoxia for 24 h. S, T: Changes in GSSG levels in liver and LYCF cells with/without hypoxia. U, V: Changes in GSH/GSSG ratio in liver and LYCF cells with/without hypoxia. *: $P<0.05$; **: $P<0.01$.

hypoxic stress is dependent on the deactivation of mitochondrial complex I in the ETC. In addition, Lu et al. (2012) found that superoxide in rat hippocampal slices in response to hypoxic stress is derived from the NOX complex. Given that excessive ROS is a mediator of hypoxic oxidative toxicity, exploring the sources of ROS in an organism under hypoxia may provide new insights to reduce hypoxic toxicity. However, to the best of our knowledge, research on the sources of excessive ROS induced by environmental hypoxia in marine fish has not been reported. In the present study,

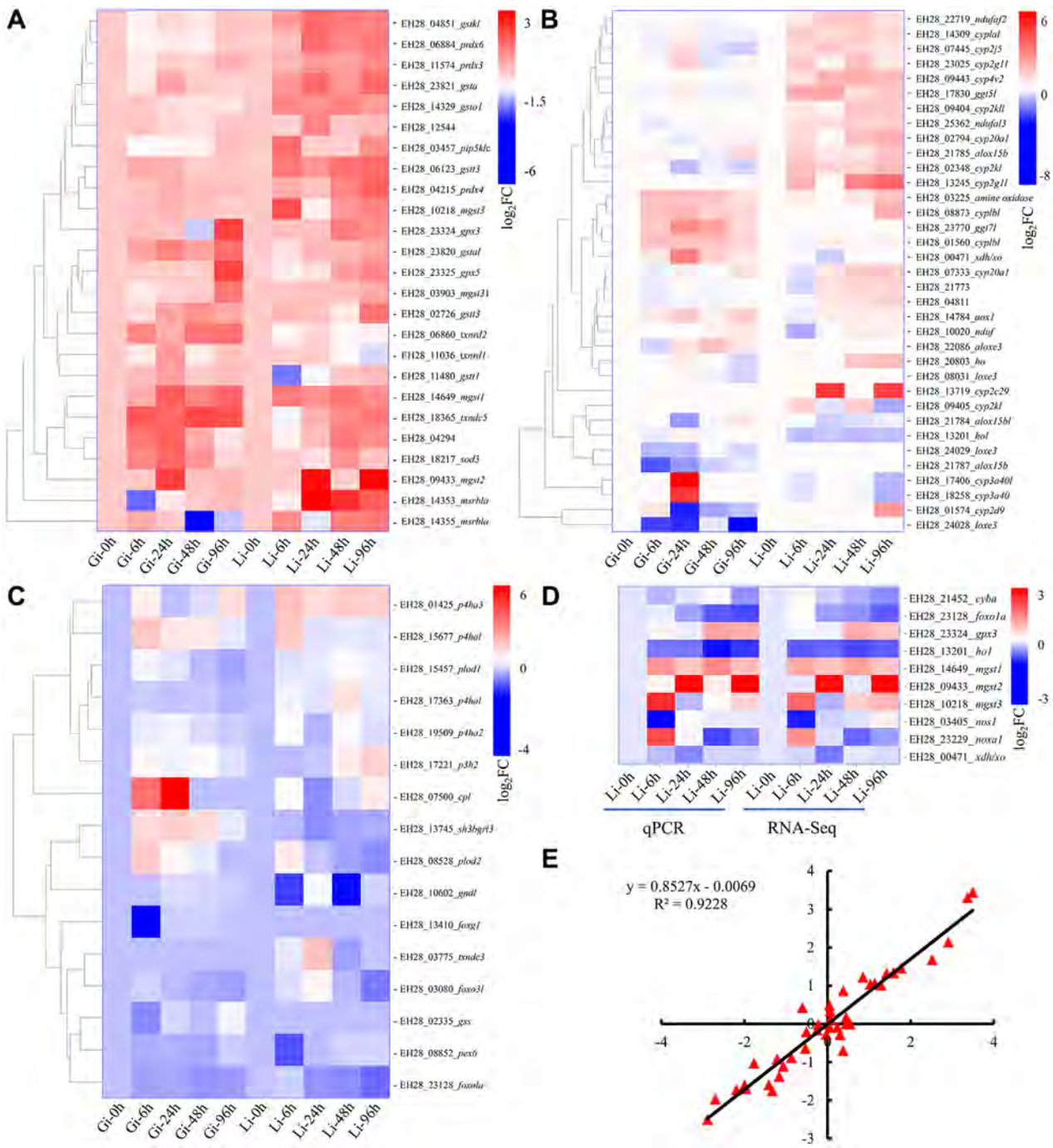

Figure 4 RNA-seq and RT-qPCR analyses characterize dynamic expression patterns of numerous key redox-related genes

A: Transcripts encoding antioxidant enzymes. B: Transcripts encoding proteins related to ROS production. C: Transcripts encoding redox-regulatory factors. D: Expression levels (log_2FC) of selected DETs determined by RT-qPCR and RNA-Seq. E: Correlation of log_2FC between RT-qPCR assay (x-axis) and RNA-seq (y-axis).

separate inhibition of ROS derived from the NOX complex and mitochondrial ETC pathways significantly reduced the levels of ROS and superoxide in the LYCF cells under hypoxic stress. Furthermore, after blocking the NOX complex and mitochondrial ETC pathways, the levels of ROS and superoxide in the hypoxia group LYCF cells recovered to the levels found in the normoxia control group. These findings indicate that excessive ROS caused by hypoxia in LYCF cells is mainly derived from mitochondrial ETC and NOX complexes rather than other cellular systems. Thus, this study provides new insight into the origins of excessive ROS in marine fish under hypoxia. However, the sources of ROS overproduction at the *in vivo* level in *L. crocea* under hypoxic stress need to be further investigated.

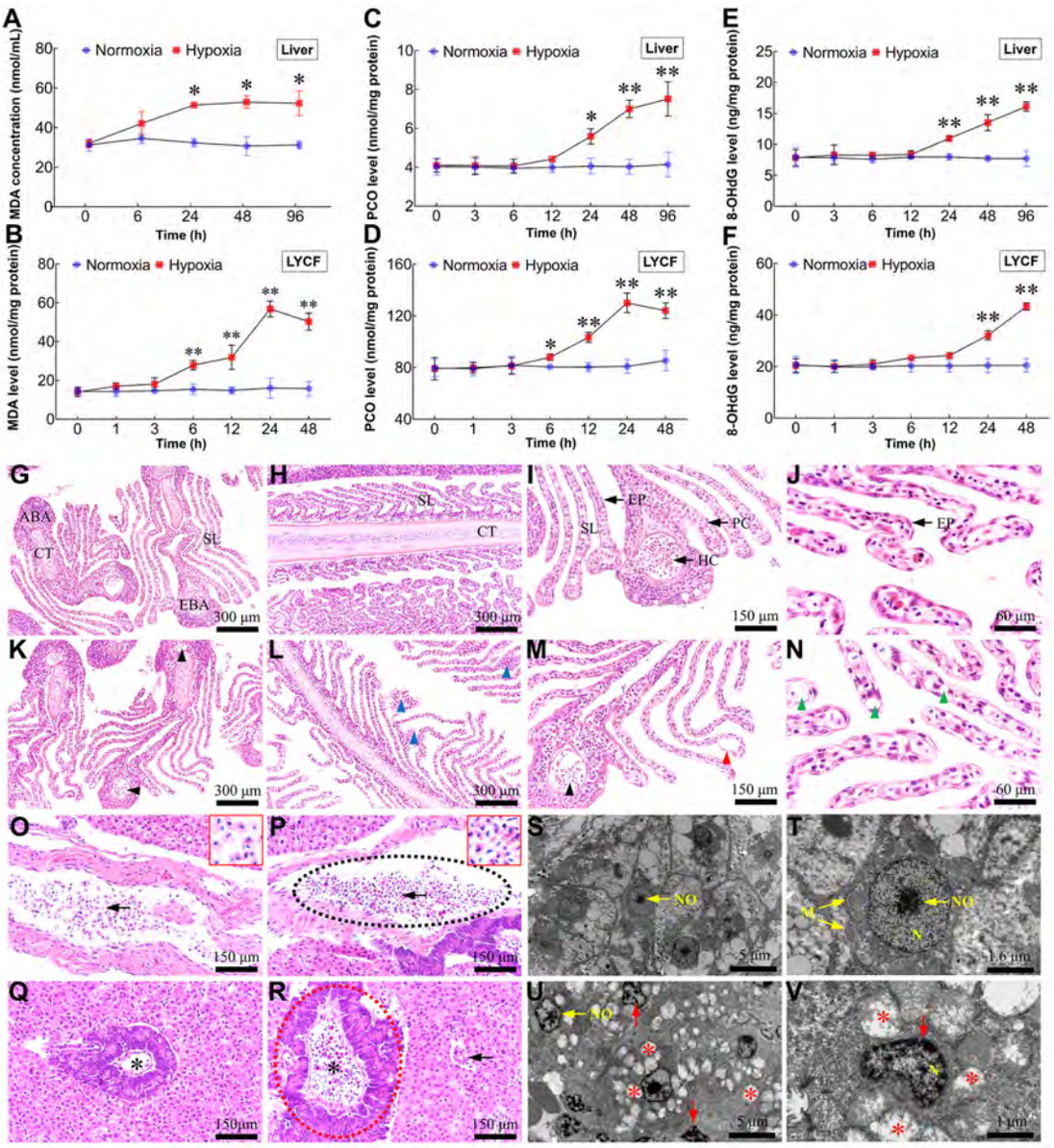

Figure 5 Excessive ROS leads to lipid peroxidation, protein carbonylation, DNA oxidation, histopathological changes, and cellular lesions

A, B: Changes in MDA levels in liver and LYCF cells with/without hypoxia. C, D: Changes in PCO levels in liver and LYCF cells with/without hypoxia. E, F: Changes in 8-OHdG levels in liver and LYCF cells with/without hypoxia. Light micrograph sections show histological structures of gills from *L. crocea* under normoxic (G, H, I, and J) and hypoxic conditions (K, L, M, and N). NCGs show different components of gill filaments with normal architecture, including cartilage tissue (CT), secondary lamellae (SL), pillar cell (PC), epithelial cell (EP), efferent branchial artery (EBA), hemocyte (HC), and afferent branchial artery (ABA). HTGs show abnormal filaments; some PCs demonstrated vacuolation (green arrowhead); HCs in ABAs and EBAs decreased (black arrowhead); PCs were shed from SL (red arrowhead); partial SL were fused (blue arrowhead). G, K, I, and M show cross-section of gill filament; H, L, J, and N show vertical section of gill filament. Light micrograph sections show histological structures of *L. crocea* livers under normoxia (O, Q) and hypoxia (P, R). Sections from NCGs (O, Q) show normal histology, compactly arranged hepatocytes, and vessels filled with normally shaped HCs (arrow). Sections from HTGs (2.0 mg/L for 96 h; P, R) show HCs in some blood vessels are unevenly distributed and stacked together (intermittent black elliptical circle). Shape of HCs and their nuclei changed from rounded to elongated (arrow). Pancreas showed partial swelling (intermittent red elliptical circle) and number of HCs increased (asterisk). S, T: Hepatic ultrastructure in NCGs was normal, exhibiting normal mitochondria with clear cristae, and rounded and centralized nuclei and nucleoli. U, V: Pathological changes were observed in samples taken from HTGs, including regression of cristae in mitochondria, resulting in mitochondrial vacuolation (asterisk), deformed nuclei, and uneven chromatin distribution (red arrow). N (nucleus); NO (nucleoli); M (mitochondria). Red-bordered boxes in O and P show magnification of HCs. *: $P<0.05$; **: $P<0.01$.

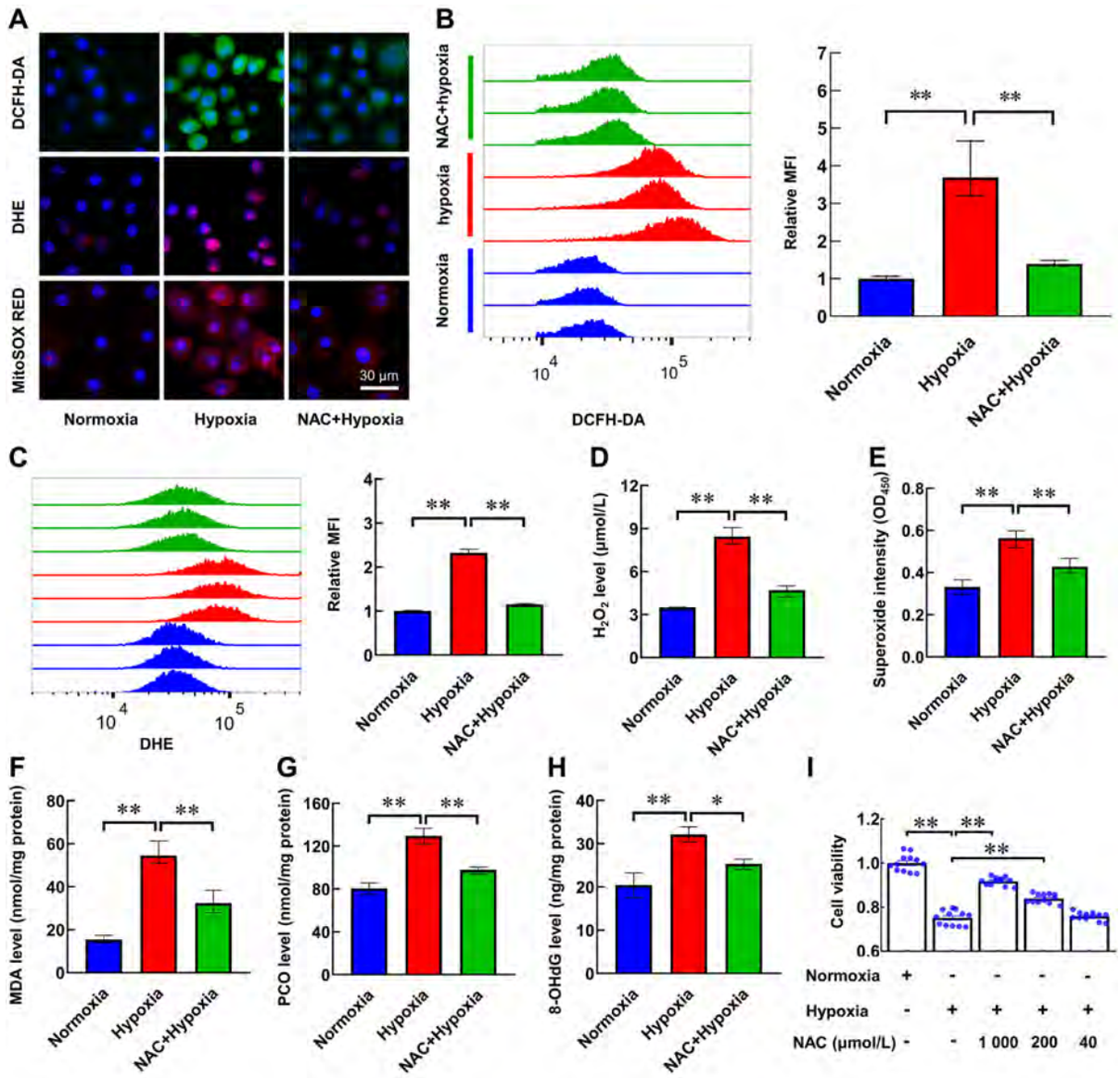

Figure 6 NAC scavenges excessive ROS in LYCF cells exposed to hypoxia, alleviates oxidative toxicity, and promotes cell viability

A: Representative fluorescence photomicrographs of ROS (DCFH-DA, green), $O_2^{\bullet-}$ (DHE, red), and mitochondrial superoxide levels (MitoSOX RED, red) in LYCF cells with/without NAC pretreatment or hypoxia for 24 h. B, C: FACS analysis of ROS and $O_2^{\bullet-}$ levels in LYCF cells with/without NAC pretreatment or hypoxia for 24 h. D: H_2O_2 assay of changes in H_2O_2 levels in LYCF cells with/without NAC pretreatment or hypoxia for 24 h. E: Superoxide assay of changes in intracellular superoxide levels in LYCF cell with/without NAC pretreatment or hypoxia for 24 h. F–H: MDA, PCO, and 8-OHdG levels in LYCF cells with/without NAC pretreatment or hypoxia for 24 h. I: Viability of LYCF cells with/without 1 mmol/L/200 μmol/L/40 μmol/L NAC pretreatment or hypoxia for 24 h. *: P<0.05; **: P<0.01.

ROS are recognized as essential “second messengers” in many cellular signaling processes (Hansen et al., 2016; Tezel, 2006). However, excessive ROS production is a trigger for oxidative damage to biomolecules. ROS can be neutralized by enzymatic or non-enzymatic reactions (Nordberg & Arnér, 2001). In our study, the remarkable rise in SOD, CAT, GPx, POD, GST, and GR activities induced by hypoxia demonstrated that environmental hypoxia activates the enzymatic antioxidant defense system in *L. crocea*. Similar results have been reported in several other fish studies. Yang et al. (2021) reported that SOD activity in *Phoxinus lagowskii* liver is significantly elevated under hypoxic stress. Zhao et al. (2020) reported that SOD and CAT activities first increase then decrease in the gills and livers of *Micropterus salmoides* exposed to environmental hypoxia. Yang et al. (2017) found that CAT and GPx activities are significantly enhanced in the liver and muscle of *M. salmoides* under acute hypoxic stress. Zhang et al. (2016) reported that GR and GST activities in the liver of *Pelteobagrus vachelli* are significantly increased under acute hypoxic stress. In addition, in the current study, many antioxidant genes, such as *sod3*, *gpx3*, *gpx5*, *grx1*, *grx5*, *prdx3*, *prdx4*, *prdx6*, *pxdn*, *txnrd1*, *txnrd2*, *txndc3*, *txndc5*,

msrb1a, *srxn1*, and *gsts*, were identified as DETs in response to hypoxia, further indicating that the enzymatic antioxidant defense system was globally activated in *L. crocea* under hypoxic stress. GSH is an important non-enzymatic antioxidant in living organisms and plays a vital role in the antioxidant defense system. Under stress conditions, GSH reacts with H_2O_2 in the presence of GPx to produce O_2 and GSSG in an organism (Labunskyy et al., 2014). In addition, GSSG is catalyzed by GR to produce GSH (Couto et al., 2016). In the present study, the decreases in the GSH level and GSH/GSSG ratio indicate that GSH was gradually depleted as a reducing substrate during antioxidation. Similarly, Wischhusen et al. (2020) reported that GSH levels are significantly reduced in rainbow trout (*Oncorhynchus mykiss*) fry under hypoxic stress.

The high levels of ROS observed in our *in vivo* and *in vitro* hypoxia models indicated that the antioxidant defense system did not successfully counteract super-abundant ROS. There is no doubt that high levels of ROS adversely affect organisms, with high levels of MDA, PCO, and 8-OHdG induced by excessive ROS widely reported (Gong et al., 2017; Gurunathan et al., 2020; Mukhopadhyay et al., 2012). In this study, the high levels of MDA, PCO, and 8-OHdG indicate that the hypoxia-induced excessive ROS impaired the plasma membrane, proteins, and genome DNA, leading to oxidative stress. Similar reports on oxidative stress caused by hypoxia have been described in other fish species. For example, Zhao et al. (2020) reported that under hypoxic stress, MDA levels in the gill and liver of *M. salmoides* increase significantly; Rahman & Thomas (2017) revealed that PCO levels are significantly higher in the brains and livers of Atlantic croaker fish collected from hypoxic regions than from normoxic regions; Mustafa et al. (2011) found that the level of DNA damage in erythrocytes of common carp (*Cyprinus carpio* L.) is significantly increased after 24 h of hypoxic stress (1.8 mg/L); Lushchak et al. (2005) reported that the levels of lipid peroxide thiobarbituric acid reactive substance (TBARS) are significantly higher in the liver of common carp in response to environmental hypoxia.

Kim et al. (2007) reported that an imbalance in ROS homeostasis can lead to mitochondrial damage, resulting in the production and release of ROS due to mitochondrial dysfunction, forming a harmful cycle and inducing further imbalance in intracellular ROS homeostasis. In the present study, we observed mitochondrial vacuolization in many *L. crocea* hepatocytes after hypoxic stress for 96 h. This may be due to excessive ROS induced by hypoxic stress attacking the mitochondria, with the damaged mitochondria producing more ROS, thus exacerbating oxidative stress and eventually leading to cell and tissue damage.

The above results demonstrate that redox balance is crucial for the adaptation of *L. crocea* to hypoxia. Interventions targeting ROS are a promising approach for improving hypoxia tolerance. NAC, a cell-permeable precursor of GSH (Viscomi et al., 2010), prevents GSH depletion and induces GPx activity (Kigawa et al., 2000; Mani et al., 2006; Saxena et al., 2019) and has been used as a generic antioxidant to reduce total ROS (Ezeriņa et al., 2018). In the present study, we found that NAC effectively mitigated hypoxia-induced ROS overproduction, reduced MDA, PCO, and 8-OHdG levels, and enhanced cell viability. Thus, removal of excessive ROS could effectively alleviate the oxidative toxicity caused by hypoxia. Similar studies on the antioxidant effects of NAC have been reported in fish cells. Chang et al. (2011) found that NAC pre-treatment can significantly reduce ROS production induced by red-spotted grouper nervous necrosis virus in a grouper fin cell line in zebrafish. Selvaraj et al. (2012) found that NAC can effectively block As_2O_3-induced intracellular ROS production in *Poeciliopsis lucida* hepatocellular carcinoma line 1 (PLHC-1) cells. Liu et al. (2017) found that NAC can lower ROS levels in the epithelioma papulosum cyprini cells of carp after spring viraemia of carp virus infection, which usually results in a time-dependent increase in ROS generation.

In addition to NAC, there are many other ROS inhibitors, such as apocynin, DPI, SS-31, and 5-HD. Apocynin and DPI limit the production of ROS by inhibiting NOX activity; apocynin inhibits NOX complex assembly (Drummond et al., 2011; Suzuki et al., 2013) and DPI functions as a flavoprotein inhibitor that reduces all NOXs (Lu et al., 2017). SS-31 targets the mitochondrial inner membrane to reduce ROS in mitochondria under physiological and pathological conditions (Szeto, 2008; Zhao et al., 2004) and 5-HD is a specific inhibitor of mitochondrial adenosine triphosphate-sensitive potassium (mitoK ATP) channel, thus preventing mitochondrial ROS production (Doughan et al., 2008). Datta et al. (2009) reported that NAC, apocynin, and DPI all exert antioxidant effects in *Clarias batrachus*. Domarecka et al. (2020) showed that apocynin has antioxidant and anti-apoptotic properties in zebrafish. In this study, the levels of ROS and superoxide in the LYCF cells were significantly lower in the hypoxia+apocynin, hypoxia+DPI, hypoxia+SS-31, and hypoxia+5-HD groups compared with the hypoxia group, indicating that apocynin, DPI, SS-31, and 5-HD can significantly reduce the levels of ROS in LYCF cells under hypoxic stress. Therefore, although cell viability and oxidative stress indices of LYCF cells after apocynin, DPI, SS-31, and 5-HD treatment and hypoxic stress were not detected in this study, we can still speculate that they may play a role in antioxidation and assist in maintaining ROS homeostasis in marine fish.

In conclusion, our findings demonstrated that environmental hypoxia induced considerable ROS production via the ETC and NOX complex pathways in *L. crocea*. Although the cellular redox homeostasis regulatory system was initiated, the amount of ROS exceeded its regulatory capability and induced oxidative stress, which caused cellular lesions, decreased cell viability, and histological damage. Modifiers targeting ROS, such as NAC, apocynin, DPI, SS-31, and 5-HD, effectively reduced ROS overproduction and alleviated its adverse effects on cells (Figure 7). Consequently, appropriate use of ROS scavengers (e.g., NAC and SS-31) or inhibitors (e.g., apocynin, DPI, and 5-HD) may be a potentially effective strategy to enhance hypoxia tolerance in *L. crocea*. This study provides insights into previously unstudied strategies for

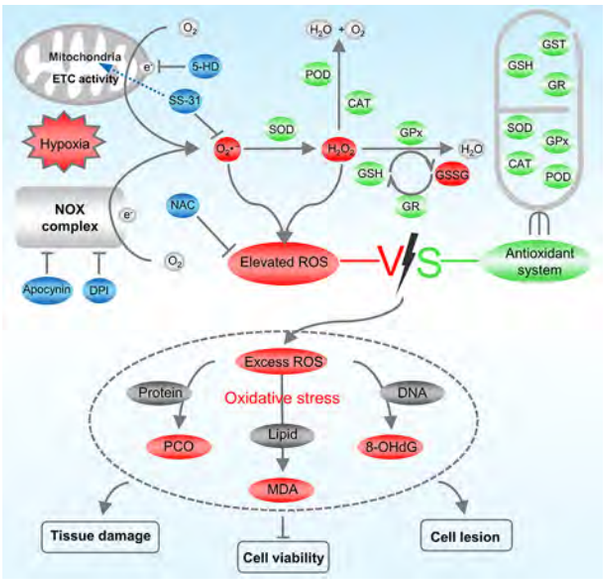

Figure 7 Regulation mode of ROS inhibitor on redox homeostasis in *Larimichthys crocea* under hypoxic stress

Hypoxia induces *L. crocea* to produce excessive $O_2^{\bullet -}$ through mitochondrial ETC and NOX complex pathways. $O_2^{\bullet -}$ is reduced to H_2O_2 by SOD enzymes, H_2O_2 is reduced to H_2O and O_2 by CAT and POD enzymes and reacts with GSH substrate and GPx enzymes to produce GSSG. GR is responsible for reduction in GSSG to GSH to continue its antioxidant action. Antioxidant defense system is activated but fails to remove excessive ROS in time, which attacks proteins, lipids, and DNA in the organism, triggering oxidative stress and causing tissue and cell damage. Apocynin and DPI prevent ROS production by inhibiting NOX complex. SS-31 enters mitochondrial inner membrane to specifically scavenge mitochondrial ROS. 5-HD inhibits production of mitochondrial ROS by specifically inhibiting mitoK ATP.

overcoming hypoxic toxicity in marine fish and ways in which to improve farming efficiency of economically valuable species.

SUPPLEMENTARY DATA

Supplementary data to this article can be found online.

COMPETING INTERESTS

The authors declare that they have no competing interests.

AUTHORS' CONTRIBUTIONS

S.Y.L., C.L., J.D., Y.B,Z., C.D., C.C.H., J.Q.Z., and B.L. designed the research. S.Y.L., C.L., J.D., J.Q.W., and Y.B.Z. performed the research. S.Y.L., J.D., X.M.G., and J.Q.Z. analyzed the data. S.Y.L. and J.Q.Z. wrote the paper. S.Y.L., C.L., X.M.G., J.Q.W., C.D., C.C.H., J.Q.Z., X.F.W., and W.L.S. modified the manuscript. All authors read and approved the final version of the manuscript.

ACKNOWLEDGMENTS

The authors thank Dr. You-Hua Huang for providing the LYCF cell line. The authors would also like to thank Editage (www.editage.cn) for English language editing.

REFERENCES

Almeida AS, Figueiredo-Pereira C, Vieira HLA. 2015. Carbon monoxide and mitochondria-modulation of cell metabolism, redox response and cell death. *Frontiers in Physiology*, **6**: 33.

Baldissera MD, de Freitas Souza C, Boaventura TP, Nakayama CL, Baldisserotto B, Luz RK. 2020. Involvement of the phosphoryl transfer network in gill bioenergetic imbalance of pacamã (*Lophiosilurus alexandri*) subjected to hypoxia: notable participation of creatine kinase. *Fish Physiology and Biochemistry*, **46**(1): 405−416.

Balogh E, Tóth A, Méhes G, Trencsényi G, Paragh G, Jeney V. 2019. Hypoxia triggers osteochondrogenic differentiation of vascular smooth muscle cells in an HIF-1 (hypoxia-inducible factor 1)-dependent and reactive oxygen species-dependent manner. *Arteriosclerosis, Thrombosis, and Vascular Biology*, **39**(6): 1088−1099.

Breitburg D, Levin LA, Oschlies A, Grégoire M, Chavez FP, Conley DJ, et al. 2018. Declining oxygen in the global ocean and coastal waters. *Science*, **359**(6371): eaam7240.

Brownlee M. 2005. The pathobiology of diabetic complications: a unifying mechanism. *Diabetes*, **54**(6): 1615−1625.

Chang CW, Su YC, Her GM, Ken CF, Hong JR. 2011. Betanodavirus induces oxidative stress-mediated cell death that prevented by anti-oxidants and *zf*catalase in fish cells. *PLoS One*, **6**(10): e25853.

Couto N, Wood J, Barber J. 2016. The role of glutathione reductase and related enzymes on cellular redox homoeostasis network. *Free Radical Biology and Medicine*, **95**: 27−42.

Datta S, Mazumder S, Ghosh D, Dey S, Bhattacharya S. 2009. Low concentration of arsenic could induce caspase-3 mediated head kidney macrophage apoptosis with JNK–p38 activation in *Clarias batrachus*. *Toxicology and Applied Pharmacology*, **241**(3): 329−338.

DeCoursey TE. 2016. The intimate and controversial relationship between voltage-gated proton channels and the phagocyte NADPH oxidase. *Immunological Reviews*, **273**(1): 194−218.

Diaz RJ. 2001. Overview of hypoxia around the world. *Journal of Environmental Quality*, **30**(2): 275−281.

Ding J, Liu C, Luo SY, Zhang YB, Gao XM, Wu XF, et al. 2020. Transcriptome and physiology analysis identify key metabolic changes in the liver of the large yellow croaker (*Larimichthys crocea*) in response to acute hypoxia. *Ecotoxicology and Environmental Safety*, **189**: 109957.

Domarecka E, Skarzynska M, Szczepek AJ, Hatzopoulos S. 2020. Use of zebrafish larvae lateral line to study protection against cisplatin-induced ototoxicity: a scoping review. *International Journal of Immunopathology and Pharmacology*, **34**: 2058738420959554.

Doughan AK, Harrison DG, Dikalov SI. 2008. Molecular mechanisms of angiotensin II-mediated mitochondrial dysfunction: linking mitochondrial oxidative damage and vascular endothelial dysfunction. *Circulation Research*, **102**(4): 488−496.

Drummond GR, Selemidis S, Griendling KK, Sobey CG. 2011. Combating oxidative stress in vascular disease: NADPH oxidases as therapeutic targets. *Nature Reviews Drug Discovery*, **10**(6): 453−471.

Ezeriņa D, Takano Y, Hanaoka K, Urano Y, Dick TP. 2018. N-acetyl cysteine functions as a fast-acting antioxidant by triggering intracellular H_2S and sulfane sulfur production. *Cell Chemical Biology*, **25**(4): 447−459.e4.

Fishery Administration of the Ministry of Agriculture and Rural Areas,

National Fisheries Technology Extension Center, China Society of Fisheries. 2020. China Fishery Statistical Yearbook 2020. Beijing: China Agricultural Press. (in Chinese)

Fransen M, Nordgren M, Wang B, Apanasets O. 2012. Role of peroxisomes in ROS/RNS-metabolism: implications for human disease. *Biochimica et Biophysica Acta (BBA) - Molecular Basis of Disease*, **1822**(9): 1363−1373.

Gimenez M, Schickling BM, Lopes LR, Miller FJ Jr. 2016. Nox1 in cardiovascular diseases: regulation and pathophysiology. *Clinical Science*, **130**(3): 151−165.

Gong YS, Hu K, Yang LQ, Guo J, Gao YQ, Song FL, et al. 2017. Comparative effects of EtOH consumption and thiamine deficiency on cognitive impairment, oxidative damage, and β-amyloid peptide overproduction in the brain. *Free Radical Biology and Medicine*, **108**: 163−173.

Guérin P, El Mouatassim S, Ménézo Y. 2001. Oxidative stress and protection against reactive oxygen species in the pre-implantation embryo and its surroundings. *Human Reproduction Update*, **7**(2): 175−189.

Gurunathan S, Jeyaraj M, Kang MH, Kim JH. 2020. Melatonin enhances palladium-nanoparticle-induced cytotoxicity and apoptosis in human lung epithelial adenocarcinoma cells A549 and H1229. *Antioxidants*, **9**(4): 357.

Guzy RD, Hoyos B, Robin E, Chen H, Liu LP, Mansfield KD, et al. 2005. Mitochondrial complex III is required for hypoxia-induced ROS production and cellular oxygen sensing. *Cell Metabolism*, **1**(6): 401−408.

Hansen T, Galougahi KK, Celermajer D, Rasko N, Tang O, Bubb KJ, et al. 2016. Oxidative and nitrosative signalling in pulmonary arterial hypertension — Implications for development of novel therapies. *Pharmacology & Therapeutics*, **165**: 50−62.

Hernansanz-Agustín P, Ramos E, Navarro E, Parada E, Sánchez-López N, Peláez-Aguado L, et al. 2017. Mitochondrial complex I deactivation is related to superoxide production in acute hypoxia. *Redox Biology*, **12**: 1040−1051.

Holowiecki A, O'Shields B, Jenny MJ. 2017. Spatiotemporal expression and transcriptional regulation of heme oxygenase and biliverdin reductase genes in zebrafish (*Danio rerio*) suggest novel roles during early developmental periods of heightened oxidative stress. *Comparative Biochemistry and Physiology Part C: Toxicology & Pharmacology*, **191**: 138−151.

Jastroch M, Divakaruni AS, Mookerjee S, Treberg JR, Brand MD. 2010. Mitochondrial proton and electron leaks. *Essays in Biochemistry*, **47**: 53−67.

Kigawa G, Nakano H, Kumada K, Kitamura N, Takeuchi S, Hatakeyama T, et al. 2000. Improvement of portal flow and hepatic microcirculatory tissue flow with N-acetylcysteine in dogs with obstructive jaundice produced by bile duct ligation. *The European Journal of Surgery*, **166**(1): 77−84.

Kim I, Rodriguez-Enriquez S, Lemasters JJ. 2007. Selective degradation of mitochondria by mitophagy. *Archives of Biochemistry and Biophysics*, **462**(2): 245−253.

Klein JA, Ackerman SL. 2003. Oxidative stress, cell cycle, and neurodegeneration. *The Journal of Clinical Investigation*, **111**(6): 785−793.

Labunskyy VM, Hatfield DL, Gladyshev VN. 2014. Selenoproteins: molecular pathways and physiological roles. *Physiological Reviews*, **94**(3): 739−777.

Leng N, Dawson JA, Thomson JA, Ruotti V, Rissman AI, Smits BMG, et al. 2013. EBSeq: an empirical bayes hierarchical model for inference in RNA-seq experiments. *Bioinformatics*, **29**(8): 1035−1043.

Leonarduzzi G, Sottero B, Poli G. 2010. Targeting tissue oxidative damage by means of cell signaling modulators: the antioxidant concept revisited. *Pharmacology & Therapeutics*, **128**(2): 336−374.

Leung TM, Nieto N. 2013. CYP2E1 and oxidant stress in alcoholic and non-alcoholic fatty liver disease. *Journal of Hepatology*, **58**(2): 395−398.

Liu L, Tu X, Shen YF, Chen WC, Zhu B, Wang GX. 2017. The replication of spring viraemia of carp virus can be regulated by reactive oxygen species and NF-κB pathway. *Fish & Shellfish Immunology*, **67**: 211−217.

Liu W, Liu XX, Wu CW, Jiang LH. 2018. Transcriptome analysis demonstrates that long noncoding RNA is involved in the hypoxic response in *Larimichthys crocea*. *Fish Physiology and Biochemistry*, **44**(5): 1333−1347.

Lu JM, Risbood P, Kane CT Jr, Hossain MT, Anderson L, Hill K, et al. 2017. Characterization of potent and selective iodonium-class inhibitors of NADPH oxidases. *Biochemical Pharmacology*, **143**: 25−38.

Lu Q, Wainwright MS, Harris VA, Aggarwal S, Hou YL, Rau T, et al. 2012. Increased NADPH oxidase-derived superoxide is involved in the neuronal cell death induced by hypoxia-ischemia in neonatal hippocampal slice cultures. *Free Radical Biology and Medicine*, **53**(5): 1139−1151.

Luo SY, Gao XM, Ding J, Liu C, Du C, Hou CC, et al. 2019. Transcriptome sequencing reveals the traits of spermatogenesis and testicular development in large yellow croaker *(Larimichthys crocea*). *Genes*, **10**(12): 958.

Lushchak VI, Bagnyukova TV, Lushchak OV, Storey JM, Storey KB. 2005. Hypoxia and recovery perturb free radical processes and antioxidant potential in common carp (*Cyprinus carpio*) tissues. *The International Journal of Biochemistry & Cell Biology*, **37**(6): 1319−1330.

Mahfouz ME, Hegazi MM, El-Magd MA, Kasem EA. 2015. Metabolic and molecular responses in Nile tilapia, *Oreochromis niloticus* during short and prolonged hypoxia. *Marine and Freshwater Behaviour and Physiology*, **48**(5): 319−340.

Mani AR, Ippolito S, Ollosson R, Moore KP. 2006. Nitration of cardiac proteins is associated with abnormal cardiac chronotropic responses in rats with biliary cirrhosis. *Hepatology*, **43**(4): 847−856.

Martínez ML, Raynard EL, Rees BB, Chapman LJ. 2011. Oxygen limitation and tissue metabolic potential of the African fish *Barbus neumayeri*: roles of native habitat and acclimatization. *BMC Ecology*, **11**(1): 2.

Meneshian A, Bulkley GB. 2002. The physiology of endothelial xanthine oxidase: from urate catabolism to reperfusion injury to inflammatory signal transduction. *Microcirculation*, **9**(3): 161−175.

Ming JH, Ye JY, Zhang YX, Yang X, Shao XP, Qiang J, et al. 2019. Dietary optimal reduced glutathione improves innate immunity, oxidative stress resistance and detoxification function of grass carp (*Ctenopharyngodon idella*) against microcystin-LR. *Aquaculture*, **498**(1): 594−605.

Mukhopadhyay P, Horváth B, Zsengellér Z, Bátkai S, Cao ZX, Kechrid M, et al. 2012. Mitochondrial reactive oxygen species generation triggers inflammatory response and tissue injury associated with hepatic ischemia-reperfusion: therapeutic potential of mitochondrially targeted antioxidants. *Free Radical Biology and Medicine*, **53**(5): 1123−1138.

Mustafa SA, Al-Subiai SN, Davies SJ, Jha AN. 2011. Hypoxia-induced oxidative DNA damage links with higher level biological effects including specific growth rate in common carp, *Cyprinus carpio* L. *Ecotoxicology*, **20**(6): 1455−1466.

Nordberg J, Arnér ESJ. 2001. Reactive oxygen species, antioxidants, and the mammalian thioredoxin system. *Free Radical Biology and Medicine*, **31**(11): 1287−1312.

Oró D, Yudina T, Fernández-Varo G, Casals E, Reichenbach V, Casals G, et al. 2016. Cerium oxide nanoparticles reduce steatosis, portal

hypertension and display anti-inflammatory properties in rats with liver fibrosis. *Journal of Hepatology*, **64**(3): 691−698.

Pacher P, Beckman JS, Liaudet L. 2007. Nitric oxide and peroxynitrite in health and disease. *Physiological Reviews*, **87**(1): 315−424.

Rahman MS, Thomas P. 2011. Characterization of three IGFBP mRNAs in Atlantic croaker and their regulation during hypoxic stress: potential mechanisms of their upregulation by hypoxia. *American Journal of Physiology: Endocrinology and Metabolism*, **301**(4): E637−E648.

Rahman MS, Thomas P. 2017. Molecular and biochemical responses of hypoxia exposure in Atlantic croaker collected from hypoxic regions in the northern Gulf of Mexico. *PLoS One*, **12**(9): e0184341.

Saxena S, Vekaria H, Sullivan PG, Seifert AW. 2019. Connective tissue fibroblasts from highly regenerative mammals are refractory to ROS-induced cellular senescence. *Nature Communications*, **10**(1): 4400.

Schulte PM. 2014. What is environmental stress? Insights from fish living in a variable environment. *Journal of Experimental Biology*, **217**(1): 23−34.

Selvaraj V, Yeager-Armstead M, Murray E. 2012. Protective and antioxidant role of selenium on arsenic trioxide-induced oxidative stress and genotoxicity in the fish hepatoma cell line PLHC-1. *Environmental Toxicology and Chemistry*, **31**(12): 2861−2869.

Sommer N, Pak O, Schörner S, Derfuss T, Krug A, Gnaiger E, et al. 2010. Mitochondrial cytochrome redox states and respiration in acute pulmonary oxygen sensing. *European Respiratory Journal*, **36**: 1056−1066.

Sommer N, Strielkov I, Pak O, Weissmann N. 2016. Oxygen sensing and signal transduction in hypoxic pulmonary vasoconstriction. *European Respiratory Journal*, **47**(1): 288−303.

Suzuki S, Pitchakarn P, Sato S, Shirai T, Takahashi S. 2013. Apocynin, an NADPH oxidase inhibitor, suppresses progression of prostate cancer via Rac1 dephosphorylation. *Experimental and Toxicologic Pathology*, **65**(7–8): 1035−1041.

Szeto HH. 2008. Mitochondria-targeted cytoprotective peptides for ischemia-reperfusion injury. *Antioxidants & Redox Signaling*, **10**(3): 601−619.

Tezel G. 2006. Oxidative stress in glaucomatous neurodegeneration: mechanisms and consequences. *Progress in Retinal and Eye Research*, **25**(5): 490−513.

Viscomi C, Burlina AB, Dweikat I, Savoiardo M, Lamperti C, Hildebrandt T, et al. 2010. Combined treatment with oral metronidazole and N-acetylcysteine is effective in ethylmalonic encephalopathy. *Nature Medicine*, **16**(8): 869−871.

Wang QF, Shen WL, Hou CC, Liu C, Wu XF, Zhu JQ. 2017. Physiological responses and changes in gene expression in the large yellow croaker *Larimichthys crocea* following exposure to hypoxia. *Chemosphere*, **169**: 418−427.

Waypa GB, Chandel NS, Schumacker PT. 2001. Model for hypoxic pulmonary vasoconstriction involving mitochondrial oxygen sensing. *Circulation Research*, **88**(12): 1259−1266.

Wischhusen P, Larroquet L, Durand T, Oger C, Galano JM, Rocher A, et al. 2020. Oxidative stress and antioxidant response in rainbow trout fry exposed to acute hypoxia is affected by selenium nutrition of parents and during first exogenous feeding. *Free Radical Biology and Medicine*, **155**: 99−113.

Yang S, Yan T, Wu H, Xiao Q, Fu HM, Luo J, et al. 2017. Acute hypoxic stress: effect on blood parameters, antioxidant enzymes, and expression of *HIF-1alpha* and *GLUT-1* genes in largemouth bass (*Micropterus salmoides*). *Fish & Shellfish Immunology*, **67**: 449−458.

Yang YT, Wang Z, Wang J, Lyu FM, Xu KX, Mu WJ. 2021. Histopathological, hematological, and biochemical changes in high-latitude fish *Phoxinus lagowskii* exposed to hypoxia. *Fish Physiology and Biochemistry*, **47**(4): 919−938.

Zhang GS, Mao JQ, Liang FF, Chen JW, Zhao C, Yin SW, et al. 2016. Modulated expression and enzymatic activities of Darkbarbel catfish, *Pelteobagrus vachelli* for oxidative stress induced by acute hypoxia and reoxygenation. *Chemosphere*, **151**: 271−279.

Zhao KS, Zhao GM, Wu DL, Soong Y, Birk AV, Schiller PW, et al. 2004. Cell-permeable peptide antioxidants targeted to inner mitochondrial membrane inhibit mitochondrial swelling, oxidative cell death, and reperfusion injury. *The Journal of Biological Chemistry*, **279**(33): 34682−34690.

Zhao LL, Cui C, Liu Q, Sun JL, He K, Adam AA, et al. 2020. Combined exposure to hypoxia and ammonia aggravated biological effects on glucose metabolism, oxidative stress, inflammation and apoptosis in largemouth bass (*Micropterus salmoides*). *Aquatic Toxicology*, **224**: 105514.